

**CONTINUED CYTOADHERENCE OF *PLASMODIUM FALCIPARUM* INFECTED
RED BLOOD CELLS AFTER ANTIMALARIAL TREATMENT**

Names: Katie R. Hughes*, Giancarlo A. Biagini and Alister G. Craig

Address: Liverpool School of Tropical Medicine, Pembroke Place, Liverpool, L3 5QA,
UK

Running Title: Cytoadherence of drug treated *P. falciparum*

Abbreviations: iRBC, Infected red blood cells; PfEMP-1, Plasmodium falciparum erythrocyte membrane protein 1; DBL, Duffy binding like; ICAM-1, intercellular adhesion molecule 1; CSA, chondroitin sulphate A; HUVEC, human umbilical vein endothelial cells; HDMEC, human dermal microvascular endothelial cells; TNF, tumour necrosis factor; FACS, fluorescence activated cell sorter

*Corresponding author: krhughes@liverpool.ac.uk

Keywords: malaria; endothelial; pathogenesis; adhesion; ICAM-1; artemisinin; quinine

Text Word Count: ~4500

Abstract Word Count: 200

Number of Figures: 5 (Plus 2 Supplementary)

Number of tables: (1 Supplementary)

Number of References: 42

ABSTRACT

Development of severe disease in *Plasmodium falciparum* malaria infection is thought to be, at least in part, due to sequestration of trophozoite-stage infected red blood cells in the microvasculature. The process of cytoadherence is mediated by binding of the parasite protein PfEMP-1 on the surface of infected red blood cells to endothelial cell receptors. Although antimalarial treatments rapidly kill parasites, significant mortality is still seen in severe malaria, particularly within 24 hours of hospital admission. We find that cytoadherence of infected red blood cells continues for several hours after killing of the parasite by antimalarials; after 24 hours treatment using a range of antimalarials binding is approximately one third the level of untreated parasite cultures. This is consistent with maintained presence of PfEMP-1 on the surface of drug-treated infected red blood cells. A specific advantage of artesunate over other treatments tested is seen on addition of this drug to younger ring stage parasites, which do not mature to the cytoadherent trophozoite-stage. These findings show that cytoadherence, a potentially pathogenic property of *P. falciparum* infected red blood cells, continues long after the parasite has been killed. These data support the development of adjunctive therapies to reverse the pathophysiological consequences of cytoadherence.

INTRODUCTION

Plasmodium falciparum malaria is responsible for over a million deaths a year ¹ with many of these fatalities occurring in infants in Africa. An important aspect of the pathogenesis of severe malaria results from the ability of infected red blood cells to sequester in the microvasculature. During the 48 h parasite growth stage inside a host red blood cell the parasite makes many changes to the cell. As well as becoming more metabolically active, and more rigid, the infected red blood cell becomes capable of adhering to the endothelial cells lining the blood vessels ². Post-

mortem studies of severe malaria show high levels of infected red blood cells (iRBC) bound to microvasculature ^{3,4}. The involvement of sequestration in pathogenesis could be directly a result of blocking of the blood vessels, and/or downstream effects caused by the interaction between iRBC and the endothelium, including local inflammatory responses ⁵.

Cytoadherence is mediated by a parasite protein PfEMP-1 which is a large protein comprising several external Duffy-binding-like (DBL) domains, encoded for by *var* genes. *P. falciparum* has around 60 *var* genes, of which only one is expressed at a time. This process of antigenic variation is a way in which the parasite evades recognition by host adaptive antibody immune responses and the large number of variants of PfEMP-1 also results in the potential to bind to many different host receptors ⁶.

Of the fourteen cell adhesion receptors to which iRBC can bind, a few have been well characterized including ICAM-1, CD36 and Chondroitin Sulfate A (CSA). ICAM-1 is of interest as it is linked to cerebral malaria ⁷. Patients suffering with cerebral malaria have up-regulated levels of ICAM-1 in the brain and parasite isolates from patients suffering from cerebral malaria show higher binding to ICAM-1 protein ^{8,9}. CD36 is expressed on many types of endothelia (but negligibly in the brain) and has the ability to bind most patient isolates. Adhesion to endothelium devoid of CD36 may be possible using platelets expressing CD36 as a bridging interaction ¹⁰. The carbohydrate CSA is uniquely implicated in placental adhesion during pregnancy. Parasites able to adhere to CSA express an unusually conserved PfEMP-1 which is expressed during malaria in pregnancy ¹¹.

It is known that cytoadherence of iRBC induces signalling events in endothelial cells^{12,13}. Some of these signalling responses may help protect the host endothelium against damage, as suggested by the down-regulation of apoptotic genes in endothelial cells¹⁴. However, other effects may be damaging. For example, the induction of ICAM-1 expression on endothelial cells occurs in response to iRBCs¹⁴, which could lead to further sequestration of iRBC, as well as local leukocyte recruitment, amplifying pathology caused by adhesion or local inflammatory responses. There is also evidence of induction of apoptosis and leakage in endothelial cells following adhesion of iRBC¹⁵.

Antimalarial treatments are effective at killing parasites where resistance has not developed; however, there is still a high mortality rate associated with severe malaria with most deaths occurring in the first 24 h after hospital admission¹⁶. It is clear that even after initiation of antimalarial treatment, patients continue to manifest worrying clinical signs¹⁶. One hypothesis, tested in this study, is that non-viable parasites killed by standard antimalarial treatment contribute to disease pathology by their continued ability to cytoadhere. To investigate this phenomenon, we have performed *in vitro* assays for cytoadherence with drug-treated *P. falciparum* iRBCs to ICAM-1 and human endothelium under both static and flow conditions.

Using a range of antimalarials we show that non-viable *P. falciparum* iRBCs retain the ability to cytoadhere at least 24 h after drug administration as a result of the slow rate of degradation of the surface protein PfEMP-1.

MATERIALS AND METHODS

Parasite Strains and Culture

Parasite lines ItG¹⁷ and A4¹⁸ were used in this study. Both of these strains are of the IT lineage and are well characterized for their ability to bind to ICAM-1 and CD36¹⁹. ItG was selected on ICAM-1 protein and expression of the expected *var* gene confirmed by cloning and sequencing a DBL α tag from cDNA. A4 was selected for binding to the monoclonal antibody BC6²⁰ followed by immunofluorescence analysis (IFA) of expressed PfEMP-1 and sequencing of the expressed *var* tag. Populations used were >80% homogeneous for the expected *var* tag. Parasites were cultured under standard conditions in RPMI 1640 medium (supplemented with 37.5 mM HEPES, 7 mM D-glucose, 6 mM NaOH, 25 $\mu\text{g ml}^{-1}$ gentamicin sulphate, 2 mM L-glutamine and 10% human serum) at a pH of 7.2, in a gas mixture of 96% nitrogen, 3% carbon dioxide and 1% oxygen²¹ and synchrony maintained using sorbitol lysis at ring stages²². Two cultures were maintained in parallel 24 h apart to allow stage-matched controls for 24 hour time point experiments.

Qualitative and quantitative measurement of PfEMP-1 levels of the surface of *P. falciparum* A4 iRBCs

PfEMP-1 on the surface of live A4 iRBC was visualised by immunofluorescence using BC6 monoclonal primary antibody (1:50 dilution), a secondary rabbit anti-mouse antibody (serotec) (1:100) followed by Alexa488 conjugated goat anti-rabbit antibody (molecular probes) (1:5000). All washes and antibody dilutions were in Dulbecco's PBS with 1% BSA and each incubation was at 37°C for 30 min. Infected cells were stained with ethidium bromide (1 $\mu\text{g/ml}$), mounted on a microscope slide and analysed by confocal microscopy using Zeiss LSMPascal microscope and Zeiss Pascal and Photoshop software (Adobe). For flow cytometry analysis staining was carried out as above then infected cells were diluted in PBS and 500,000 events (red blood cells) acquired on Beckman Coulter FACS XL, gated using forward scatter and side scatter to acquire red blood cell populations excluding debris and then FL-1 and FL-2 fluorescence intensity measured. Analysis was performed using WinMDi

software. Regions were drawn on density plots (i.e. Fig 4 b) of uninfected controls to gate uninfected cells such that <0.1% of the population fell into the region classed as ethidium bromide positive. This region was then used to create a histogram. Region R1 was created for A4var41 positive cells based on negative antibody controls, <0.1% of the ethidium bromide positive population fell into region R1 when no primary antibody was included. Similarly for the antigenically distinct strain ItG <0.1% of the ethidium bromide positive population fell into region R1 (not shown). The mean fluorescence intensity (MFI) of region R1 was used to quantitate the level of PfEMP-1 on A4var41 positive infected red blood cells. The percentage of A4 iRBC that were classed as A4var41 positive remained at ~80%.

Endothelial Cells

Human umbilical vein endothelial cells (HUVEC) and human dermal microvascular endothelial cells (HDMEC) were purchased from Promocell and cultured as per manufacturer's instructions. Cells at passage 4 to 6 were used for all experiments. Prior to experimentation cells were stimulated by the addition of 1 ng/ml TNF for 18 hours. This procedure allowed for the induction of ICAM-1 expression on the surface of the endothelial cells as verified by immunofluorescence microscopy and flow cytometry after immunofluorescence (data not shown).

Adhesion assays

All adhesion assays were carried out essentially as previously described¹⁹. In brief:

Flow Based Protein Assays

Aminopropyltriethoxysilane (APES) treated microslides were coated with ICAM-1-Fc²³ protein at 50 µg/ml in Dulbecco's PBS. Protein was allowed to adhere for 2 h, then slides were washed with 1% BSA/PBS and blocked in 1% BSA/PBS overnight at 4°C. Parasites were prepared to 3% parasitaemia and 1% haematocrit (hct) in

binding buffer (RPMI 1640 medium pH 7.2, supplemented with 6 mM glucose). After flowing binding medium through the microslide for 2 min, prepared parasites were flowed through at a pump speed of 0.186 ml/min, to give a wall shear stress of 0.05 Pa, for 5 minutes. This was followed by flowing binding buffer for 2 min. All assays were carried out at 37°C. Stationary adhered parasites were counted in 6 fields along the slide. Each experiment was performed in duplicate or triplicate and on three independent occasions.

Static Endothelial Cell Assays

Endothelial cells cultured as above were seeded onto 13 mm thermanox coverslips (Nunc) coated with 1% gelatin in 24 well plates. Confluent cells were induced with 1 ng/ml TNF for 18 hours and washed in culture medium before an assay. Parasites were prepared to 1% hct and 3% parasitaemia in binding buffer. 0.5 ml of cell suspension were applied to each well and incubated at 37°C for 1 h with gentle resuspension by rotation every 10 min. Unbound cells were removed by 2 washes in binding buffer followed by 2 x 30 min gravity washes in binding buffer. Cells were fixed with 1% glutaraldehyde for ≥ 1 h. After staining with 5% Geimsa for 30 min, coverslips were washed in water, air dried and mounted using DPX hard set mounting medium. 6 – 10 areas of each cover slip were counted for the number of bound parasites. Each experiment was performed in duplicate or triplicate and on three independent occasions.

Flow Based Endothelial Cell Assays

APES treated microslides were coated with 1% gelatin, 1% collagen for 45 minutes at 37°C. Endothelial cells at passage 3–5 were treated with trypsin to detach adherent cells (Promocell detach kit used as per manufacturers' instructions). Cell suspensions were applied to the microslides, and allowed to settle for 2 h at 37°C to form a confluent monolayer. After overnight growth with media exchange every hour,

TNF (1 ng/ml) was added to the confluent cells for 18 hours before the assay. Parasites were prepared at 3% parasitaemia and 1% hct in binding buffer. After flowing binding medium through the microslide for 2 min, prepared parasites were flowed through at a wall shear stress of 0.05 Pa for 5 min, followed by a wash with binding buffer (2 min). Stationary adherent parasites were counted in at least 6 fields along the slide. Each experiment was performed in duplicate or triplicate and on three independent occasions.

Drug Treatment

The effect of parasite viability on cytoadherence was tested using a range of drugs including artesunate, quinine, lumefantrine and piperazine. Final drug concentrations were chosen based on published peak plasma levels. These were; 500nM for artesunate,^{24,25} 25µM for quinine^{26,27}, 15µM for lumefantrine^{28,29}, and 100nM for piperazine^{26,30}.

The concentrations of drugs used were well above the IC₅₀ determined for each (Table 1, supplementary information) and were confirmed to inhibit parasite development as assessed by Geimsa staining as described in the results section. Parasites were confirmed non-viable after treatment by continued culture for at least 72 h post-treatment with no growth. The minimum exposure time to 500 nM artesunate to stop parasite growth was determined to be 30 minutes. Various exposure times greater than this followed by washing out of the drug did not affect binding phenotype 24 h following treatment (Supplementary Fig S1).

Growth inhibition (IC₅₀) assays were performed on ItG and A4 parasites using a standard fluoremetric assay^{31,32}.

Statistical Analysis

Each binding experiment was performed in duplicate or triplicate and the mean calculated. Results shown are the mean of three independent experiments +/- SD.

Statistical significance was calculated using a two tailed t-test.

RESULTS

Cytoadherence of artesunate treated *P. falciparum* ItG iRBCs to ICAM-1 under flow

Adhesion of *P. falciparum* ItG iRBC to ICAM-1 protein under flow was assayed following 4, 8 and 24 h artesunate (500 nM) treatment of trophozoite (24 h post invasion) stage parasites. Parasite development as assessed by geimsa staining appeared to halt after 4 h treatment (Fig 1a) and parasites were noticeably pyknotic following 8 h treatment. As described in the Methods section, parasites were not viable for culture following drug treatment.

No significant difference in binding was observed for parasites exposed to artesunate for 4 h compared to untreated parasites (Fig. 1b). Following 8 h exposure, a slight reduction in binding was seen and following 24 h artesunate treatment adhesion to ICAM-1 was reduced to ~30% of control levels ($P < 0.01$, Fig 1). The concentration of artesunate used (500 nM) was chosen as it falls in the normal range reported for observed plasma concentrations (see Methods and Supplementary Table 1), however, similar binding phenotypes were observed for artesunate concentrations ranging from 20 nM to 12.5 μ M (Supplementary Fig S2).

Cytoadherence of artesunate treated *P. falciparum* ItG iRBCs to human endothelial cells

Adhesion of *P. falciparum* ItG iRBCs to human endothelial cells (HUVEC and HDMEC) was assessed under both static and flow conditions following 4, 8 and 24 h artesunate (500 nM) treatment of trophozoite (24 h post invasion) stage parasites.

As described in the Methods section, binding assays were performed with confluent monolayers of TNF (1 ng/ml, 18 h) activated endothelial cells. Under these

conditions HUVEC express the receptor ICAM-1, whereas HDMEC express both CD36 and ICAM-1.

Under static conditions, there was no significant difference in the level of binding to either HUVEC or HDMEC of *P. falciparum* IgG iRBCs incubated for 4 h with artesunate (500 nM) compared to the untreated controls to (Fig. 2 a,b). Following 8 h exposure, a slight reduction in binding was seen and following 24 h artesunate treatment adhesion to both HUVEC ($P<0.01$) and HDMEC ($P<0.05$) was reduced to ~30% of control levels (Fig 2a,b).

Essentially the same binding phenotypes were observed for adhesion measured under flow, with up to 8 h exposure to artesunate (500 nM) not significantly affecting adhesion to both HUVEC or HDMEC, whilst 24 h exposure to artesunate (500 nM) did reduce the levels of binding to both cell types to 25-30% of control levels (Fig. 2c,d).

Cytoadherence of other *P. falciparum* isolates to other receptors after artesunate treatment

Similar results to those seen for IgG adhesion after artesunate treatment were also seen with two other parasite isolates. A4, like IgG, binds to both ICAM-1 and CD36 but generally at lower levels than IgG¹⁹. The adhesion of A4 to ICAM-1 protein under flow and to HDMEC under static conditions was assessed. No significant reduction in adhesion was seen after 8 h treatment of trophozoite-stage parasites with artesunate (500 nM), however, after 24 hours treatment adhesion was reduced to 25-30% of controls. Additionally the CSA binding strain CS2³³ was assayed for cytoadherence to CSA protein under flow conditions. No reduction in adhesion was seen after 8 h treatment and significant adhesion at around 25% control levels was observed after

24 h treatment. Experiments after 4 and 24 h drug treatment showed that IgG binding to CD36 was similarly affected (Supplementary Fig S3)

Measurement of PfEMP-1 levels on the surface of drug treated *P. falciparum* iRBCs

To determine whether the continued ability of non-viable parasites to adhere is due to the persistence of the PfEMP-1 complex on the infected erythrocyte membrane, single cell and population immunofluorescence measurements were performed using the monoclonal antibody mAb BC6, specific for the PfEMP-1 A4var41 variant¹⁸.

Confocal laser scanning microscopy of *P. falciparum* A4 iRBCs after immunofluorescent labelling with the primary monoclonal antibody BC6 revealed the characteristic punctate distribution of PfEMP-1 on the outer erythrocytic membrane (Fig. 3a.). Qualitatively, the distribution of PfEMP-1 was not observably different in *P. falciparum* iRBCs treated for up to 24 h with 500 nM artesunate (Fig. 3a). Analysis by flow cytometry confirmed that ~80% of iRBCs expressed detectable levels of A4var41 PfEMP-1 (Fig. 3b). This population percentage did not change through the course of these experiments. Following treatment with artesunate (500 nM, 24 h), the mean fluorescence of PfEMP-1 surface positive iRBCs was reduced to approximately 65% the level of untreated cells ($P < 0.01$, $n=3$, Fig. 3c, d). Notably, PfEMP-1 could still be detected on iRBC surface after 4 days treatment (data not shown).

Cytoadherence of *P. falciparum* IgG iRBCs to ICAM-1: Comparison of antimalarials

Adhesion of *P. falciparum* IgG iRBC to ICAM-1 protein under flow was assayed following 4, 8 and 24 h drug treatment of trophozoite (24 h post invasion) stage parasites. The antimalarial drugs tested were artesunate (500 nM), quinine (25 μ M), lumefantrine (15 μ M) and piperazine (100 nM). As described in the Methods

section, all drugs were used at concentrations comparable to published peak plasma concentrations and were confirmed to result in the abrogation of parasite viability.

The binding phenotypes for all treatments were observed to be very similar, with no significant difference in binding observable after 4 h drug exposure (Fig. 4a). As observed previously, a small reduction in binding was observed for parasites exposed to 8 h artesunate (Fig. 4b) but no significant difference relative to control cells was observed for all other drugs (Fig. 4b). A significant reduction in iRBC binding was observed following 24 h exposure to all of the drugs, with binding ~30% of control levels (Fig. 4c).

Cytoadherence of *P. falciparum* ItG iRBCs to ICAM-1: Comparison of antimalarials administered to ring-stage parasites

As the antimalarial drugs used in this study have different pharmacodynamic properties, especially in regards to cell cycle specificity, binding experiments to ICAM-1 under flow conditions were repeated as described above but drug exposure was performed on ring-stage (12 h post invasion) parasite cultures. These younger ring stage parasites represent the pre-cytoadherent circulating population.

Adhesion to ICAM-1 protein under flow, was determined after 24 h exposure of ring-stage *P. falciparum* ItG iRBCs to artesunate (500 nM), quinine (25 µM), lumefantrine (15 µM) and piperazine (100 nM) relative to untreated control cells. Significant differences were observed between the various treatments. Artesunate treated parasites were unable to mature to trophozoites and non-viable ring parasites were observed after 24 h exposure (Fig. 5a), whilst quinine and lumefantrine treated parasites matured to late trophozoites before dying and appearing pyknotic (Fig. 5a). Piperazine treated parasites appeared to show an intermediate amount of development to late ring/early trophozoite before becoming non-viable. Binding

experiments revealed that control parasites allowed to develop for 24 h from ring stage parasites to trophozoites displayed characteristic levels of adhesion whilst control ring-stage parasites, as expected, displayed a very low level of cytoadherence (Fig. 5b). Artesunate treated parasites, which as described had failed to mature showed little cytoadherence, whilst quinine and lumefantrine treated parasites displayed high levels of adhesion comparable to control trophozoite-stage iRBC (Fig. 5b). Treatment of parasites with piperazine resulted in intermediate levels of binding, ~50% of control levels (Fig. 5b).

DISCUSSION

In this study we have assessed the ability of non-viable parasites killed by antimalarial treatments to cytoadhere, a process important in the pathophysiology of disease.

Our data demonstrate that *P. falciparum* iRBC are capable of cytoadherence for at least 24 h after lethal dosages of a range of antimalarial drugs. The antimalarial drugs tested in this study were artesunate, quinine, lumefantrine and piperazine at clinically relevant concentrations, chosen to mimic peak plasma drug levels. The cytoadherence phenotype of iRBCs was measured using both static and flow assays and using a range of parasite strains (ItG, A4 and CS2) against purified receptor proteins (ICAM-1, CD36 and CSA) and endothelial cells (HUVEC and HDMEC).

Consistent with the continued ability to cytoadhere, we observed the characteristic punctate distribution of PfEMP-1 on the surface of *P. falciparum* iRBC at significant levels (~65% of control) following 24 h antimalarial treatment (Fig. 3).

These data illustrate the stability of the changes made to the red blood cell by the parasite such that the remodelling of the infected red blood cells is maintained after the parasite is rendered non-viable. Nevertheless, quantification of the PfEMP-1 levels on iRBCs surface showed some reduction after drug treatment, consistent with a degree of degradation/loss of the protein. This reduction in PfEMP-1, combined with potential reduction in other cytoadherence-related parasite proteins, i.e. KAHRP, could explain the reduced levels of cytoadherence seen after 24 h treatment. This could be comparable to that seen when mutations are present in haemoglobin, i.e. haemoglobin C (HbC), and sickle haemoglobin (HbS). In these cases infected erythrocytes show a slightly reduced and abnormal display of PfEMP-1 and concurrently reduced cytoadherence³⁴.

Testing a selection of antimalarial drugs showed that the effect on mature (24 h post infection) trophozoite cytoadherence was not drug specific; the same level of adhesion was seen after 24 h treatment with all of the antimalarials tested (Fig. 3).

Previously published data has implied that antimalarial drugs including quinine, halofantrine, artesunate and artemether reduce cytoadherence and/or rosetting in *P. falciparum*³⁵. In the Udomsangpetch et al., study, parasites (presumably ring stage circulating parasites) were exposed to antimalarial drugs for 2 to 24 h, washed and grown in culture until control parasites (no drug exposure) were at late trophozoite/early schizont stage. Depending on the drug treatment these authors reported a range of binding phenotypes, most notably parasites exposed to artesunate and artemether were reported to result in ≥ 50 % inhibition of both cytoadherence (static assay) and rosetting. It was concluded by these authors that the observed differences between the various drugs on parasite adhesion probably reflected differences in the susceptibility of asexual stage parasites to antimalarials.

We show a similar effect when drug treatment is added to ring stage (young) parasites. As shown in Fig. 5a, the various antimalarials used inhibited parasite growth at different stages of the asexual cycle. This is consistent with previous pharmacodynamic data on the mode of action of these drugs. The minimum exposure time to artesunate (500 nM) to render parasites non viable was just 30 minutes, reflecting the fast mode of action of this drug upon activation of the endoperoxide bridge^{36,37}. Furthermore the drug is known to be active against young ring stage parasites. The activity of lumefantrine, quinine and piperazine, however, is based on the disruption of heme detoxification^{38,39} occurring later in development during haemoglobin digestion by trophozoite stage parasites^{36,40,41}. The pharmacodynamic differences of these drugs when administered to ring stage

parasites results in mismatched comparisons of binding phenotypes. Essentially the assays measured the adhesion of dead ring stage parasites for the artesunate treated group, against the adhesion of dead trophozoite stage parasites for the quinine, lumefantrine and piperaquine treated groups (Fig. 5a,b). The significant reduction in adhesion seen by artesunate treated parasites in Fig. 5 and in the Udomsangpetch et al., study³⁵ simply reflect that these groups consist of ring stage parasites that have insufficient levels of binding proteins, i.e. PfEMP-1, exported to the erythrocyte membrane surface at that stage.

The significant observation of our study is that dead parasites retain the ability to cytoadhere irrespective of the antimalarial treatment administered. However, we can hypothesise that administration of fast, ring stage acting antimalarials such as artesunate will result in a reduction of *de novo* cytoadherence when administered *in vivo* due to their ability to prevent maturation of parasites to mature cytoadherent stages. The persistence of cytoadherence for many hours after treatment, despite rapid effects on parasite viability fits with, and may in part explain, the clinical observation of a high (84 % in one study) mortality rate in first 24 hours after hospital admission after initiation of antimalarial treatment¹⁶. Even though treatment is killing the parasites rapidly, we show that they would still be able to cytoadhere 24 h following treatment, potentially still contributing to disease pathology.

It is conceivable that the observed phenomenon of continued adherence by non-viable *P. falciparum* iRBCs may be targeted by adjuvant therapies designed to prevent or preferably reverse cytoadherence. Indeed, studies have recently been performed with Levamisole, which was shown to reduce sequestration of *P. falciparum* in patients by inhibition of CD36 dephosphorylation⁴².

In summary, this study has assessed the cytoadherence capability of drug-killed *P. falciparum* iRBCs. Our data demonstrate that non-viable parasites, irrespective of treatment retain the ability to cytoadhere for up to 24 h. This phenomenon is due to the stability of the changes made to the host red blood cell by the parasite, as illustrated by the continued presence of PfEMP-1 on the surface of iRBC after loss of parasite viability. This continued capacity for cytoadherence could contribute to disease pathology following treatment. It is hypothesised that fast and ring stage acting antimalarials such as the endoperoxides may be therapeutically more favourable by their ability to prevent *de novo* adhesion, but adjunctive therapy strategies that can also reverse cytoadherence may also be advantageous in addressing the high mortality seen in severe malaria early after hospital admission

Acknowledgements

This work was supported by an MRC DTA studentship to KH and the Wellcome Trust. The authors would like to thank Tadge Szeszak for preparation of the ICAM-1-Fc protein. The authors also wish to thank the staff and patients of Ward 7Y and the Gastroenterology Unit, Royal Liverpool Hospital, for their generous donation of blood.

Authorship

GAB and AGC designed the research; KRH performed the research; all three authors analysed and interpreted the data and co-wrote the manuscript.

REFERENCES

1. Snow RW, Guerra CA, Noor AM, Myint HY, Hay SI. The global distribution of clinical episodes of *Plasmodium falciparum* malaria. *Nature*. 2005;434:214-217.
2. Cooke BM, Mohandas N, Coppel RL. The malaria-infected red blood cell: structural and functional changes. *Adv Parasitol*. 2001;50:1-86.
3. Taylor TE, Fu WJ, Carr RA, et al. Differentiating the pathologies of cerebral malaria by postmortem parasite counts. *Nat Med*. 2004;10:143-145.
4. Turner G. Cerebral malaria. *Brain Pathol*. 1997;7:569-582.
5. Chakravorty SJ, Hughes KR, Craig AG. Host response to cytoadherence in *Plasmodium falciparum*. *Biochem Soc Trans*. 2008;36:221-228.
6. Kyes SA, Kraemer SM, Smith JD. Antigenic variation in *Plasmodium falciparum*: gene organization and regulation of the var multigene family. *Eukaryot Cell*. 2007;6:1511-1520.
7. Chakravorty SJ, Craig A. The role of ICAM-1 in *Plasmodium falciparum* cytoadherence. *Eur J Cell Biol*. 2005;84:15-27.
8. Turner GD, Morrison H, Jones M, et al. An immunohistochemical study of the pathology of fatal malaria. Evidence for widespread endothelial activation and a potential role for intercellular adhesion molecule-1 in cerebral sequestration. *Am J Pathol*. 1994;145:1057-1069.
9. Newbold C, Warn P, Black G, et al. Receptor-specific adhesion and clinical disease in *Plasmodium falciparum*. *Am J Trop Med Hyg*. 1997;57:389-398.
10. Wassmer SC, Lepolard C, Traore B, Pouvelle B, Gysin J, Grau GE. Platelets reorient *Plasmodium falciparum*-infected erythrocyte cytoadhesion to activated endothelial cells. *J Infect Dis*. 2004;189:180-189.
11. Rogerson SJ, Hviid L, Duffy PE, Leke RF, Taylor DW. Malaria in pregnancy: pathogenesis and immunity. *Lancet Infect Dis*. 2007;7:105-117.
12. Tripathi AK, Sullivan DJ, Stins MF. *Plasmodium falciparum*-infected erythrocytes increase intercellular adhesion molecule 1 expression on brain endothelium through NF-kappaB. *Infect Immun*. 2006;74:3262-3270.
13. Jenkins N, Wu Y, Chakravorty S, Kai O, Marsh K, Craig A. *Plasmodium falciparum* intercellular adhesion molecule-1-based cytoadherence-related signaling in human endothelial cells. *J Infect Dis*. 2007;196:321-327.
14. Chakravorty SJ, Carret C, Nash GB, Ivens A, Szeszak T, Craig A. Altered phenotype and gene transcription in endothelial cells induced by *Plasmodium falciparum* - infected red blood cells: pathogenic or protective? *Int J Parasitol*. 2007;37:975-987.
15. Medana IM, Turner GD. *Plasmodium falciparum* and the blood-brain barrier--contacts and consequences. *J Infect Dis*. 2007;195:921-923.
16. Marsh K, Forster D, Waruiru C, et al. Indicators of life-threatening malaria in African children. *N Engl J Med*. 1995;332:1399-1404.
17. Ockenhouse CF, Betageri R, Springer TA, Staunton DE. *Plasmodium falciparum*-infected erythrocytes bind ICAM-1 at a site distinct from LFA-1, Mac-1, and human rhinovirus. *Cell*. 1992;68:63-69.
18. Roberts DJ, Craig AG, Berendt AR, et al. Rapid switching to multiple antigenic and adhesive phenotypes in malaria. *Nature*. 1992;357:689-692.

19. Gray C, McCormick C, Turner G, Craig A. ICAM-1 can play a major role in mediating *P. falciparum* adhesion to endothelium under flow. *Mol Biochem Parasitol.* 2003;128:187-193.
20. Horrocks P, Pinches R, Kyes S, et al. Effect of var gene disruption on switching in *Plasmodium falciparum*. *Mol Microbiol.* 2002;45:1131-1141.
21. Trager W, Jensen JB. Human malaria parasites in continuous culture. *Science.* 1976;193:673-675.
22. Lambros C, Vanderberg JP. Synchronization of *Plasmodium falciparum* erythrocytic stages in culture. *J Parasitol.* 1979;65:418-420.
23. Craig AG, Pinches R, Khan S, et al. Failure to block adhesion of *Plasmodium falciparum*-infected erythrocytes to ICAM-1 with soluble ICAM-1. *Infect Immun.* 1997;65:4580-4585.
24. Newton PN, Barnes KI, Smith PJ, et al. The pharmacokinetics of intravenous artesunate in adults with severe *falciparum* malaria. *Eur J Clin Pharmacol.* 2006;62:1003-1009.
25. Simpson JA, Agbenyega T, Barnes KI, et al. Population pharmacokinetics of artesunate and dihydroartemisinin following intra-rectal dosing of artesunate in malaria patients. *PLoS Med.* 2006;3:e444.
26. Akoachere M, Buchholz K, Fischer E, et al. In vitro assessment of methylene blue on chloroquine-sensitive and -resistant *Plasmodium falciparum* strains reveals synergistic action with artemisinins. *Antimicrob Agents Chemother.* 2005;49:4592-4597.
27. Le Jouan M, Jullien V, Tetanye E, et al. Quinine pharmacokinetics and pharmacodynamics in children with malaria caused by *Plasmodium falciparum*. *Antimicrob Agents Chemother.* 2005;49:3658-3662.
28. McGready R, Stepniewska K, Ward SA, et al. Pharmacokinetics of dihydroartemisinin following oral artesunate treatment of pregnant women with acute uncomplicated *falciparum* malaria. *Eur J Clin Pharmacol.* 2006;62:367-371.
29. Ashley EA, Stepniewska K, Lindegardh N, et al. Pharmacokinetic study of artemether-lumefantrine given once daily for the treatment of uncomplicated multidrug-resistant *falciparum* malaria. *Trop Med Int Health.* 2007;12:201-208.
30. Davis TM, Hung TY, Sim IK, Karunajeewa HA, Ilett KF. Piperaquine: a resurgent antimalarial drug. *Drugs.* 2005;65:75-87.
31. Bennett TN, Paguio M, Gligorijevic B, et al. Novel, rapid, and inexpensive cell-based quantification of antimalarial drug efficacy. *Antimicrob Agents Chemother.* 2004;48:1807-1810.
32. Smilkstein M, Sriwilaijaroen N, Kelly JX, Wilairat P, Riscoe M. Simple and inexpensive fluorescence-based technique for high-throughput antimalarial drug screening. *Antimicrob Agents Chemother.* 2004;48:1803-1806.
33. Cooke BM, Rogerson SJ, Brown GV, Coppel RL. Adhesion of malaria-infected red blood cells to chondroitin sulfate A under flow conditions. *Blood.* 1996;88:4040-4044.
34. Cholera R, Brittain NJ, Gillrie MR, et al. Impaired cytoadherence of *Plasmodium falciparum*-infected erythrocytes containing sickle hemoglobin. *Proc Natl Acad Sci U S A.* 2008;105:991-996.
35. Udomsangpetch R, Pipitaporn B, Krishna S, et al. Antimalarial drugs reduce cytoadherence and rosetting *Plasmodium falciparum*. *J Infect Dis.* 1996;173:691-698.

36. Skinner TS, Manning LS, Johnston WA, Davis TM. In vitro stage-specific sensitivity of *Plasmodium falciparum* to quinine and artemisinin drugs. *Int J Parasitol.* 1996;26:519-525.
37. O'Neill PM, Posner GH. A medicinal chemistry perspective on artemisinin and related endoperoxides. *J Med Chem.* 2004;47:2945-2964.
38. Biagini GA, O'Neill PM, Nzila A, Ward SA, Bray PG. Antimalarial chemotherapy: young guns or back to the future? *Trends Parasitol.* 2003;19:479-487.
39. Biagini GA, O'Neill PM, Bray PG, Ward SA. Current drug development portfolio for antimalarial therapies. *Curr Opin Pharmacol.* 2005;5:473-478.
40. Hempelmann E, Motta C, Hughes R, Ward SA, Bray PG. *Plasmodium falciparum*: sacrificing membrane to grow crystals? *Trends Parasitol.* 2003;19:23-26.
41. O'Neill PM, Ward SA, Berry NG, et al. A medicinal chemistry perspective on 4-aminoquinoline antimalarial drugs. *Curr Top Med Chem.* 2006;6:479-507.
42. Dondorp AM, Silamut K, Charunwatthana P, et al. Levamisole inhibits sequestration of infected red blood cells in patients with *falciparum* malaria. *J Infect Dis.* 2007;196:460-466.

FIGURE LEGENDS

Figure 1

Phenotype of trophozoite-stage ItG iRBC after artesunate treatment. A) Geimsa stained smears of ItG infected red blood cells after 0, 4, 8, 24 hours treatment with 500 nM artesunate under culture conditions. B) Adhesion to ICAM-1 protein (50 µg/ml) under flow conditions (0.05 Pa shear stress) after 0, 4, 8 or 24 hours treatment with 500nM artesunate. Mean of three independent experiments ± standard deviation (SD). * P <0.05 ** P<0.01 compared to untreated control (c) trophozoites.

Figure 2

Adhesion of trophozoite-stage ItG iRBC to endothelial cells after 0, 4, 8 or 24 hours artesunate treatment. Binding under static conditions to A) HUVEC and B) HDMEC after TNF stimulation (1 ng/ml 18 hours) showing bound iRBC per mm² confluent endothelial cells. Binding under flow conditions to C) HUVEC and D) HDMEC after TNF stimulation of endothelial cells showing percent of control (untreated trophozoites) binding. Each represents mean of three independent experiments ± SD. * P <0.05 ** P<0.01 compared to untreated controls (c).

Figure 3

Adhesion of trophozoite-stage ItG iRBC to ICAM-1 protein under flow conditions after 4, 8 and 24 hours treatment with artesunate (art) (500 nM), quinine (quin) (25 µM), lumefantrine (lum) (15 µM) or piperazine (pip) (100 nM). Results are mean of three independent experiments ± SD.

Figure 4

Analysis of PfEMP-1 on the surface of live trophozoite-stage A4 iRBC. after immunofluorescence using the primary antibody BC6. A) Confocal fluorescence images of (i) top plane, and (ii) centre plane of BC6 fluorescence, (iii) ethidium bromide labelling of parasite, and phase contrast images (iv), after 0 (upper) 4 (middle) or 24 hours (lower) artesunate treatment. Scale bar (2 μ M) on phase contrast image. B) Quantitation of PfEMP-1 levels by flow cytometry analysis after BC6 primary antibody and Alexa488 coupled secondary antibody (FL-1, X axis) and counterstaining infected red blood cells with ethidium bromide (FL-2, Y axis). In the density plots uninfected red blood cells are the population in the lower left. Box R1 represents BC6 positive infected red blood cells. Plot i) shows 0 h culture, plot ii) shows the culture after 24 hours artesunate treatment. C) Histogram showing quantitation of BC6 positive fluorescence intensity (X axis) of the infected population (gated as ethidium bromide positive) untreated trophozoites (open black) or after artesunate (500 nM) 24 h (solid red). D) Mean fluorescence intensity (MFI) for PfEMP-1 positive population (gate R1) mean \pm SD for three independent experiments.

Figure 5

A) Geimsa stained smears of ItG iRBC 24 hours after addition of indicated drug treatment to ring stage (young) parasites. B) Adhesion to ICAM-1 protein under flow conditions 24 hours after addition of treatment to ring stage (young) parasites.

Figure S1

Trophozoite-stage ItG iRBC adhesion to ICAM-1 protein under flow conditions after artesunate treatment for 30 min to 24 hour treatment, followed by wash out of artesunate and adhesion assay 24 hours after initial drug addition (the 0 h time point). After 30 min (or longer) exposure parasites were non-viable and development

stopped as assessed by Geimsa staining. After 0 and 15 min artesunate treatment before wash out parasites had matured as untreated controls and hence were at (non-cytoadherent) ring stage 24 hours following treatment, so were not assayed. Mean of two experiments \pm SD.

Figure S2

Trophozoite-stage ItG iRBC adhesion to ICAM-1 protein under flow conditions after 6 or 24 h treatment with various concentrations of artesunate from 20 nM to 12.5 μ M. Mean of two experiments +SD

Figure S3

Adhesion of other parasite isolates and to other adhesion receptors. Adhesion of trophozoite-stage A4 iRBC after 0, 4, 8, or 24 h artesunate (500 nM) treatment to ICAM-1 protein under flow conditions (A) or to HDMEC under static conditions (B). Adhesion of trophozoite-stage CS2 iRBC to CSA under flow conditions after 0, 4, 8 or 24 h artesunate (500 nM) treatment (C). and Adhesion of trophozoite-stage ItG iRBC to CD36 protein under static conditions after 4 h or 24 h artesunate (500 nM) treatment (D).

Figure 1

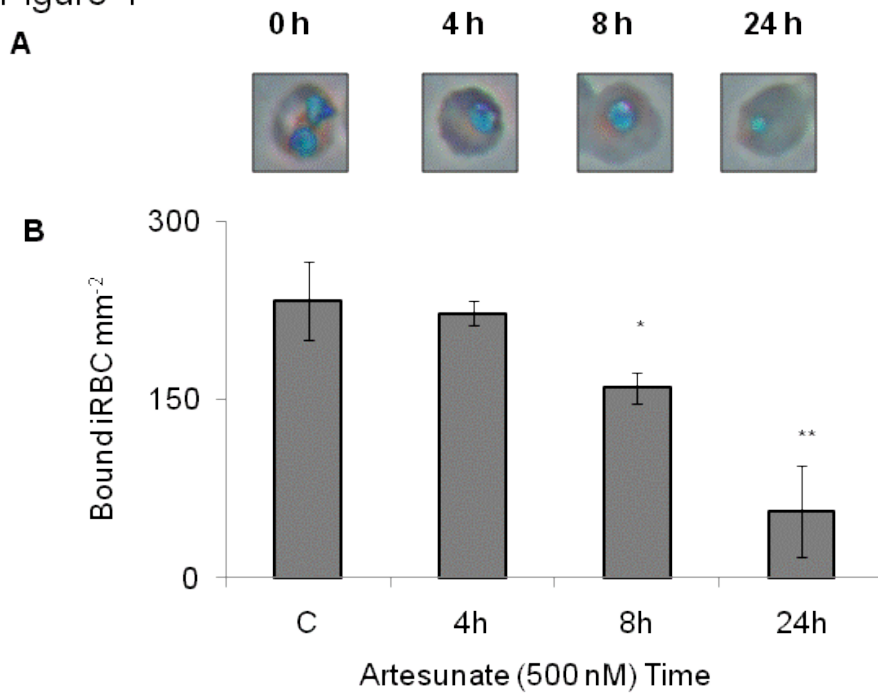


Figure 2

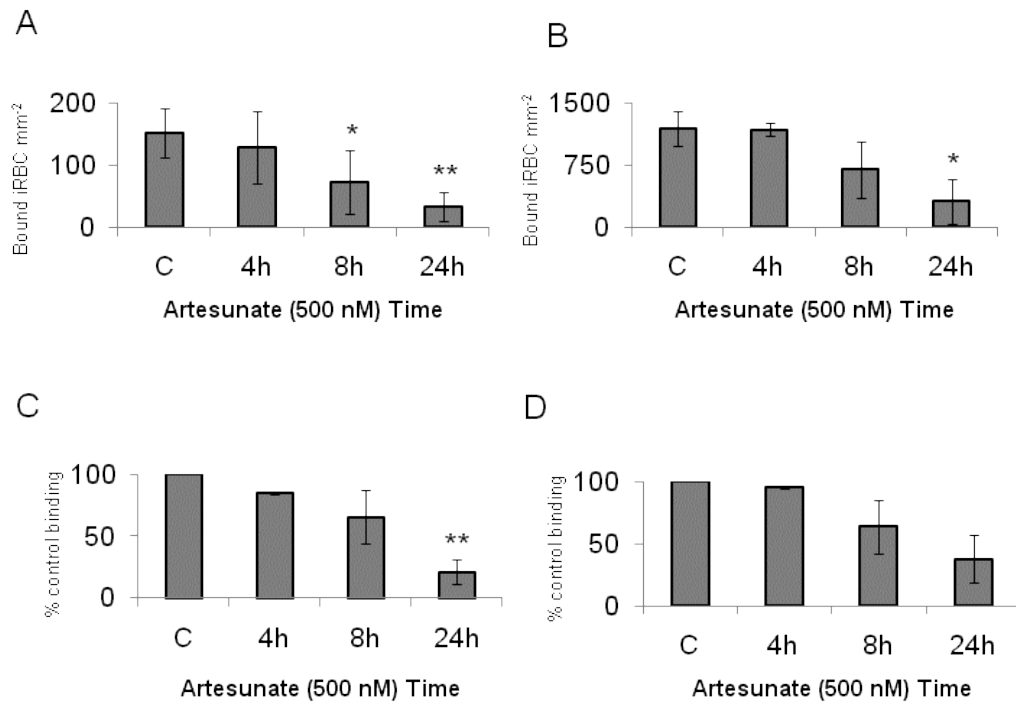


Figure 3

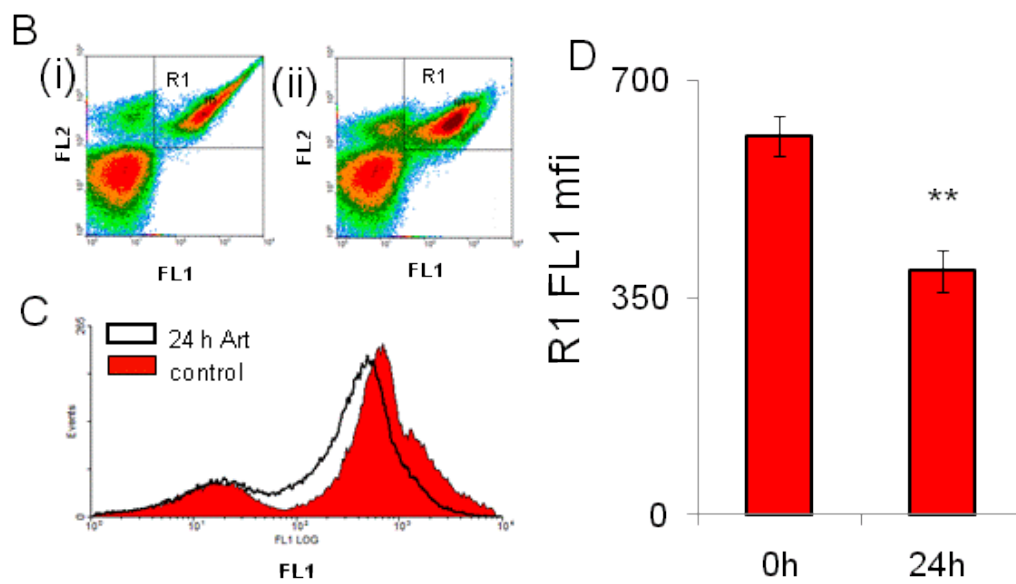
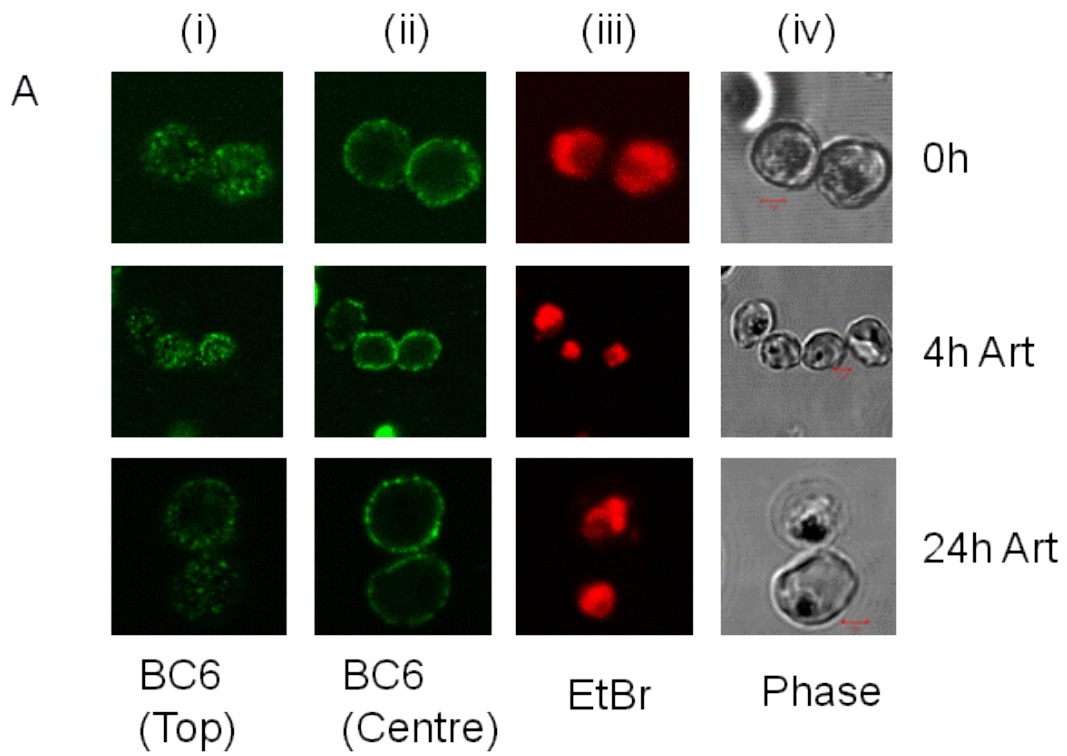


Figure 4

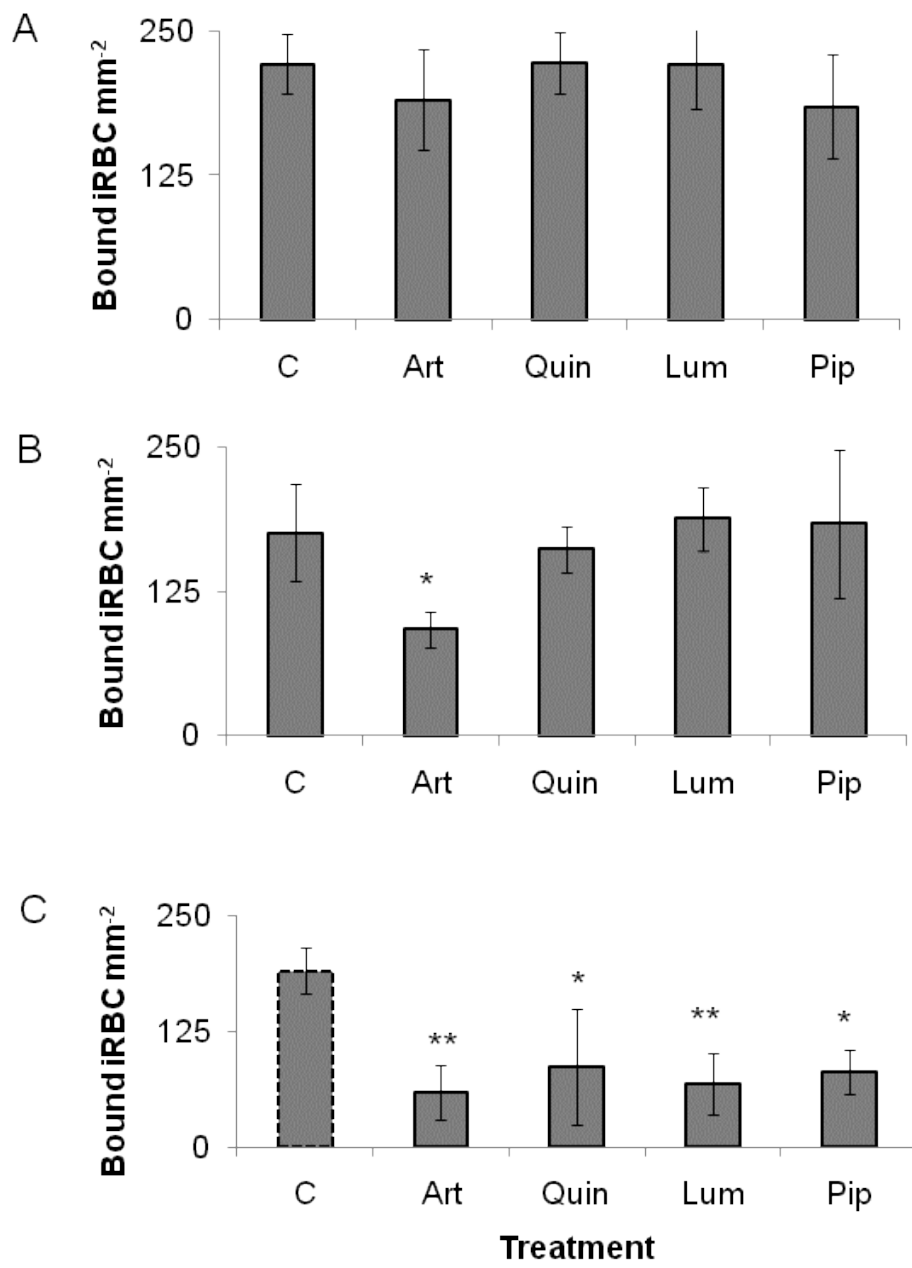
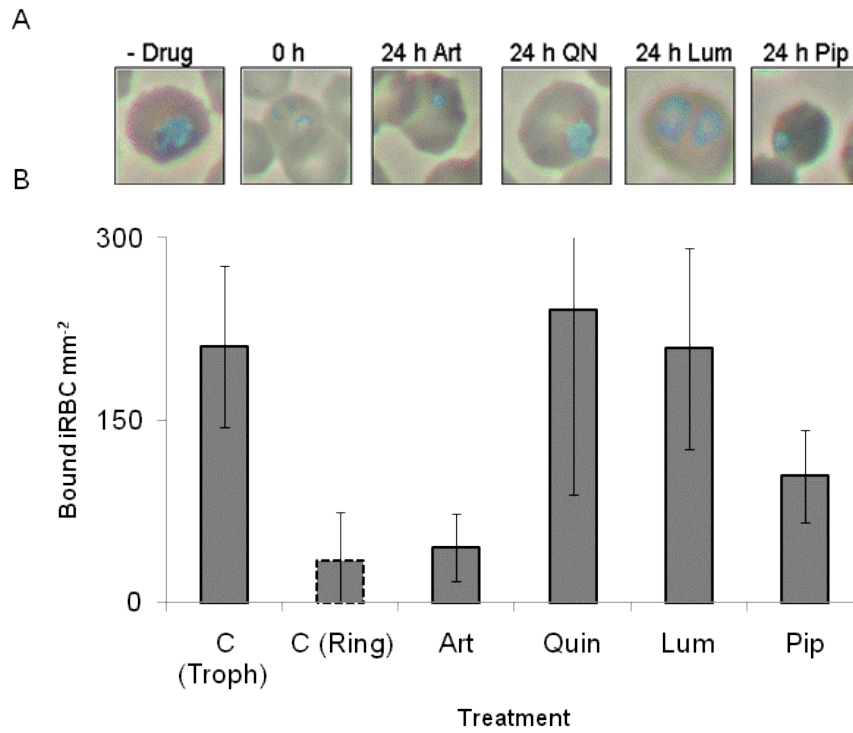


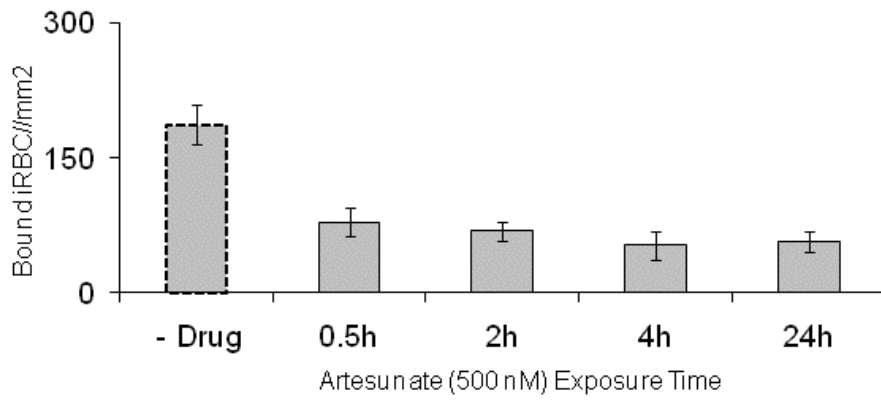
Figure 5



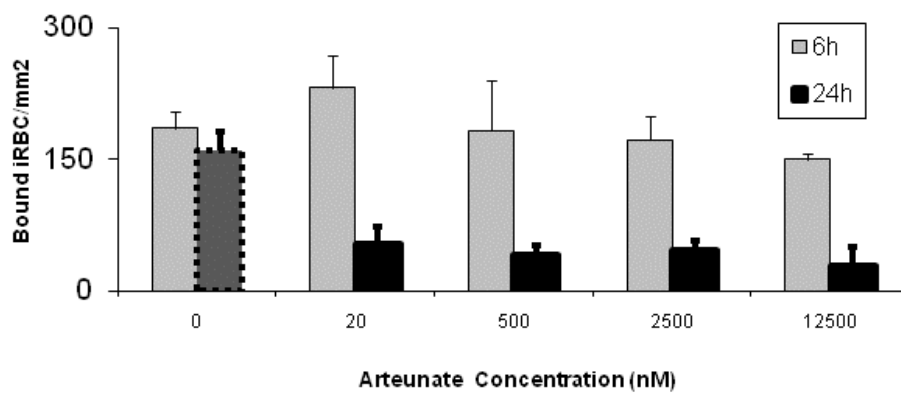
Supplementary Table 1

Drug	IC(50) on ItG Mean of three assays +/- SD	Concentration Used
Artesunate	1.6 nM +/- 1.5	500 nM
Quinine	382.48 nM +/- 140	25 μ M
Lumefantrine	233.29 nM	15 μ M
Piperaquine	52.4 nM +/- 8.16	100 nM

Supplementary Figure 1



Supplementary Figure 2



Supplementary Figure 3

